Optimisation of Copper Oxide Impregnation on Carbonised Oil Palm Empty Fruit Bunch for Nitric Oxide Removal using Response Surface Methodology

Norhidayah Ahmad[1], *Sing Hung* Yong[1], *Naimah* Ibrahim[1*], *Umi Fazara* Md Ali[1], *Fahmi* Muhammad Ridwan[1] and *Razi* Ahmad[1]

[1]School of Environmental Engineering, Universiti Malaysia Perlis, 02600 Arau, Perlis, Malaysia

Abstract. Oil palm empty fruit bunch (EFB) was successfully modified with phosphoric acid hydration followed by impregnation with copper oxide (CuO) to synthesize CuO modified catalytic carbon (CuO/EFBC) for low-temperature removal of nitric oxide (NO) from gas streams. CuO impregnation was optimised through response surface methodology (RSM) using Box-Behnken Design (BBD) in terms of metal loading (5-20%), sintering temperature (200-800˚C) and sintering time (2-6 hours). The model response for the variables was NO adsorption capacity, which was obtained from an up-flow column adsorption experiment with 100 mL/min flow of 500 ppm NO/He at different operating conditions. The optimum operating variables suggested by the model were 20% metal loading, 200˚C sintering temperature and 6 hours sintering time. A good agreement (R^2 = 0.9625) was achieved between the experimental data and model prediction. ANOVA analysis indicated that the model terms (metal loading and sintering temperature) are significant (Prob.>F less than 0.05).

1 Introduction

Nitric oxides (NO_x) is one of the major air pollutants mainly contributed from fuel combustion process in stationary and mobile sources [1-2]. NO_x causes severe environmental problems such as photochemical smog, and acid rain which are harmful to both human and environment [3]. One of the widely used methods to control NO_x is selective catalytic reduction (SCR). SCR process involves the use of catalyst system like vanadium supported on titanium oxide with external reducing agents such as NH_3 or urea to convert NO_x into N_2 and H_2O. The catalytic reaction is effective at temperature higher than 350ºC.

The use of carbonaceous materials derived from agricultural wastes in SCR of NO_x is an alternative technique that allows low temperature (100-300ºC) application. Extensive study on carbonaceous materials for NO reduction is possibly due to the material abundance and cost. Besides, carbonaceous material derived from agriculture waste shows

* Corresponding author: naimah@unimap.edu.my

high porosity and surface area which are beneficial for removal of NO_x [4]. Such materials include olive stone [5], rice husk [6], orange skin [7], palm shell [2], plum stone [8], and coconut shell [9]. In Malaysia, oil palm biomass including empty fuit bunch (EFB) is available in abundance. Hence it is very useful and economical to utilize EFB as the carbon precursor in this study.

Impregnation of additives e.g. metal catalyst on the carbonaceous material's surface is another step to enhance NO_x reduction. Copper oxide (CuO) for example was used in many studies including our previous work as it is inexpensive and exhibits high reactivity towards NO reduction [10-12]. The variables chosen in the process of CuO impregnation onto the carbonised EFB (CuO/EFBC) may affect the effectiveness of NO_x reduction, therefore, this study aims to optimise CuO impregnation using response surface method, specifically using Box–Behnken design (BBD). In this independent quadratic design, the treatment combinations are at the midpoints of edges of the process space and at the centre. BBD is favourable because less number of experimental runs is required [4].

2 Experimental

2.1 Material preparation

Fibrous oil palm EFB sample was collected from United Oil Palm Mill Sdn. Bhd., Nibong Tebal, Malaysia. The collected EFB fibre was washed with water and dried in oven at 110ºC for 24 h. The EFB was first carbonized and activated using one-stage chemical activation with phosphoric acid (H_3PO_4) at 1:1 (w/v) ratio and heated in the furnace for 24 h at 400°C to create pores, as described in previous work [10]. The heated EFB was then washed with distilled water to remove the remaining acid. Each 10 g of the carbonized material (EFBC) was further impregnated with CuO catalyst at varied loadings. Metal loading was as suggested by RSM based on minimum and maximum set of values obtained from the literature review. Then, 50 mL of distilled water was added to the mixture of EFBC and CuO and stirred with the magnetic stir bar for 4 hours. The mixture was then heated by double boiling method at 70ºC until the liquid part evaporated. After dried, the samples were sintered in the furnace at temperature and time suggested by RSM based on fixed minimum and maximum set of values. Finally, the resulting sample of CuO/EFBC was weighed and sieved to gain average particles sizes in the range of 0.5 – 1 mm for further testing.

2.2 NO removal experiment

NO adsorption experiment was explained in detailed in the previous work [10], except that the operating parameters i.e. sample loading, gas concentration and reaction temperature were changed to 5 g of CuO/EFBC, 500 ppm NO/He and 200ºC. The total gas flow rate was maintained at 100 mL/min, but passed through the packed bed reactor in an up-flow manner. Outlet NO concentration was measured by NO-NO_2 analyser (TESTO 340, Germany) at the end of the system for one hour. Differential amount of NO removed from gas stream and adsorbed by the CuO/EFBC catalyst system was measured in an experimental set-up shown in the same previous work. For the model response, NO removed from the gas streams or adsorbed by CuO/EFBC was calculated by the following equations (Eqs. 1 and 2). In this case, q was calculated using experimental NO concentration data from breakthrough curve at time equivalent, t_t, which can be obtained by integrating the fraction of NO removed ($1-C/C_o$) per minute using trapezoidal method (Eq.1) [2].

$$t_t = \int_0^\infty 1 - \frac{C}{C_o} \quad (1)$$

$$q = \frac{C_{\mathrm{NO}} Q_{\mathrm{f}} t_{\mathrm{t}} y_{\mathrm{f}}}{m_{\mathrm{c}}} \quad (2)$$

where q is adsorption capacity of NO (mg/g), C_{NO} is NO concentration (mg/L), Q_f is gas flow rate (L/min), t_t is time equivalent (min) calculated using Eq. 1, y_{f} is mole fraction of NO, and m_c is mass of adsorbent (g).

2.3 Design of Experiment

2.3.1 Experimental design

CuO impregnation variables studied include (i) x_1, metal loading; (ii) x_2, sintering temperature and (iii) x_3, sintering time, while the performance indicator or response is the NO adsorption capacity. The minimum (-1), centre (0) and maximum (1) set of values for the three variables given in Table 1 were selected based on literature and preliminary studies. A total of seventeen (17) experimental runs were suggested by RSM. The sequence of experimental run was randomized in order to minimize errors due to uncontrollable factors.

Table 1. Independent variables and their coded levels for the Box Behnken Design.

Variables			**Coded variables level**		
	Code	Unit	-1	0	1
Metal loading	x_1	%	5	12.5	20
Sintering temperature	x_2	ºC	200	400	800
Sintering time	x_3	hour	2	4	6

2.3.2 Model development

The response variables (i.e. NO adsorption capacity) obtained from the seventeen experimental runs were used to develop an empirical, quadratic model that correlates the response to the three factors, by using a second degree polynomial equation [13] given by Eq. 3.

$$Y = \beta_0 + \beta_1 x_1 + \beta_2 x_2 + \beta_3 x_3 + \beta_{12} x_1 x_2 + \beta_{13} x_1 x_3 + \beta_{23} x_2 x_3 + \beta_{11} {x_1}^2 + \beta_{22} {x_2}^2 + \beta_{33} {x_3}^2 + \varepsilon \quad (3)$$

where Y is the predicted response, β_0 is model constant, x_1, x_2, and x_3 are independent variables, β_1, β_2 and β_3 are linear coefficients, β_{12}, β_{13} and β_{23} are cross-product coefficients, β_{11}, β_{22} and β_{33} are the quadratic coefficients and ε is the statistical error term.

2.3.3 Statistical and graphical analysis

The correlation coefficient value (R^2), Fisher value (F-value) and probability (P-value) from analysis of variance (ANOVA) was used to evaluate the quality and significance of the model and model terms. Graphs were employed to analyse the combined effect of factors on the response using 3D plot and to analyse the predicted response variables versus experimental value.

2.3.4 Model optimisation and validation

Model optimisation was done to determine the optimum operating conditions for the process variables under consideration. To achieve this, goals were set based on the combined effect of factors on responses. Model validation was carried out by conducting NO removal experiment using CuO/EFBC, prepared based on optimum operating conditions suggested by the model. The experimental values (NO adsorption capacity) obtained were compared with the model predicted values.

3 Results and discussions

3.1 Development of model for optimisation of CuO impregnation

The response in term of NO adsorption capacity obtained from the seventeen experimental runs carried out according to operating variables suggested by RSM is presented in Table 2, together with the experimental design variables mentioned in Section 2.3.1.

Based on the data in Table 2, a quadratic model was developed using RSM. The final empirical model for NO adsorption was then obtained in terms of coded factors (parameters) as presented in Eq. 4.

$$Y_1 = 6.09672 \times 10^{-3} - 1.64944 \times 10^{-3} x_1 + 2.62639 \times 10^{-3} x_2 - 5.67000 \times 10^{-4} x_3 - 1.55556 \times 10^{-3} x_1x_2 + 1.01667 x_1x_3 - 4.79167 \times 10^{-7} x_2x_3 + 9.39556 \times 10^{-6} x_1^2 + 8.72222 \times 10^{-10} x_2^2 + 8.9 \times 10^{-5} x_3^2 \quad (4)$$

The fitness of the model developed was evaluated based on the correlation coefficient value (R^2) obtained from linear model extrapolation showed in Fig. 1. The R^2 value closer to unity is desirable as an indication that predicted values are closer to the actual values [14]. The R^2 value is relatively high at $R^2 = 0.9625$, indicating that there is good agreement between the adsorption capacity from experimental data and model prediction.

3.2 Statistical and graphical analysis of model

The adequacy of the model was further evaluated through analysis of variance (ANOVA). Table 3 shows the analysis done on the quadratic model for NO adsorption capacity (Y_1). Model terms, x_1, x_2, x_3 refer to metal loading, sintering temperature and sintering time.

Table 2. Experimental design matrix for optimisation of CuO impregnation onto EFBC.

Experimental Run	Variables			Response
	x_1 Metal loading (%)	x_2 Sintering temperature (°C)	x_3 Sintering time (hr)	Y Adsorption Capacity (mg/g)
1	5.0	200	4	0.00504
2	20.0	200	4	0.00614
3	5.0	800	4	0.00531
4	20.0	800	4	0.00501
5	5.0	500	2	0.00548
6	20.0	500	2	0.00576
7	5.0	500	6	0.00524
8	20.0	500	6	0.00613
9	12.5	200	2	0.00482
10	12.5	800	2	0.00539
11	12.5	200	6	0.00559
12	12.5	800	6	0.00501
13	12.5	500	4	0.00466
14	12.5	500	4	0.00479
15	12.5	500	4	0.00470
16	12.5	500	4	0.00475
17	12.5	500	4	0.00494

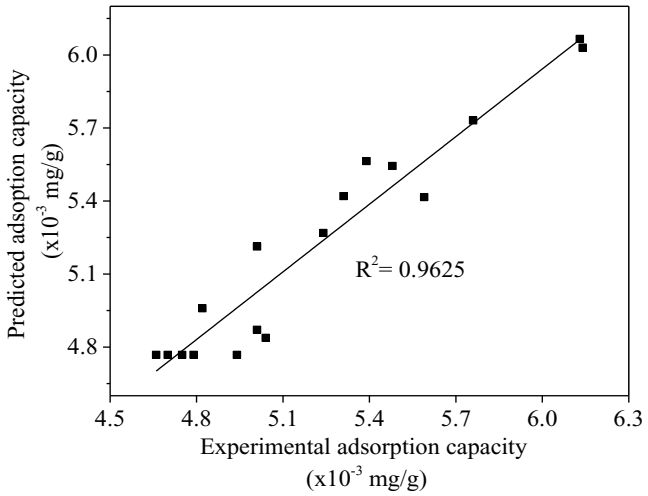

Fig. 1. Experimental and predicted values of NO adsorption capacity onto CuO/EFBC.

For the model terms, Prob. > F less than 0.05 indicates that the model term is significant [15-16] and the largest F-value indicated that the model term has the most significant effect on the response [17]. Based on Table 3, the quadratic model for adsorption capacity has an F-value of 16.24, indicating that this model is significant. In the case of model terms, x_1, x_1x_2, x_2x_3, x_1^2 and x_3^2 can be considered significant with Prob. > F values less than 0.05. However, the rest of the model terms, x_2, x_3, x_1x_3, x_2^2 are insignificant to the adsorption capacity response. The model term which has the most significant effect on the response is x_1^2 with an F-value of 50.64 and the overall effects are in the order of $x_1^2 > x_3^2 > x_1x_2 > x_1 > x_2x_3$.

Based on the results in Table 3, it is also found that the combined effects due to interactions between metal loading and sintering temperature, as well as sintering temperature and sintering time are significant to the adsorption capacity. The effect of these model terms interactions on NO adsorption capacity are shown in graphical form in Figs. 2 (a) and 2(b) using three-dimensional response surface plots.

Fig. 2(a) shows that increasing metal loading from 5 to 20% (at a constant 200ºC sintering temperature) enhances the adsorption capacity of NO from 0.00504 to 0.00614 mg/g. However, by keeping metal loading at 20%, an increase in the sintering temperature decreases the adsorption capacity from 0.00614 to 0.00501 mg/g. At the same metal loading of 5%, decreasing the sintering temperature slightly reduces the adsorption capacity from 0.00531 to 0.00504 mg/g. The interaction between high metal loading (20%) and low sintering temperature (200ºC) appears to be more effective in enhancing NO adsorption capacity. This result is in agreement with the work done by Ryu et al. [18] which reported that as the metal loading increased, the adsorption capacity increased because the surface sites for reaction increased with the increase in metal loading. Zhu et al. [19] also reported similar finding to this work.

Table 3. ANOVA analysis of NO adsorption capacity by CuO/EFBC.

Source	Sum of squares	Degree of freedom	Mean Square	F-Value	Prob.>F
Model	3.394×10^{-6}	9	3.771×10^{-7}	16.24	0.0006
x_1	4.851×10^{-7}	1	4.851×10^{-7}	20.89	0.0026
x_2	9.461×10^{-8}	1	9.461×10^{-8}	4.07	0.0833
x_3	3.380×10^{-8}	1	3.3800×10^{-9}	1.46	0.2668
x_1x_2	4.900×10^{-7}	1	4.900×10^{-7}	21.10	0.0025
x_1x_3	9.302×10^{-8}	1	9.302×10^{-8}	4.01	0.0854
x_2x_3	3.306×10^{-7}	1	3.306×10^{-7}	14.24	0.0070
x_1^2	1.176×10^{-6}	1	1.176×10^{-6}	50.64	0.0002
x_2^2	2.595×10^{-8}	1	2.595×10^{-8}	1.12	0.3256
x_3^2	5.336×10^{-7}	1	5.336×10^{-7}	22.98	0.0020

As can be observed in Fig. 2(b), at the same sintering time of 2 hrs, decreasing the sintering temperature reduced the adsorption capacity from 0.00539 to 0.00482 mg/g, while increasing sintering time from 2 to 6 hrs (at a constant 200ºC sintering temperature) increased the adsorption capacity of NO from 0.00482 to 0.00539 mg/g. For a constant 6 hrs sintering time, higher temperature decreased the adsorption capacity from 0.00539 to 0.00501 mg/g. Therefore, the interaction between high sintering time (6 hrs) and low sintering temperature (200ºC) appears to be more effective in enhancing NO adsorption capacity. Prolonged sintering time is expected to allow impregnation of more catalyst on the surface of carbon. The impregnation of catalyst increased the catalytic activity,

therefore resulted in higher adsorption capacity [20]. On the other hand, increasing the sintering temperature reduced the adsorption capacity because high sintering temperature destroys the activated carbon porous structures [21].

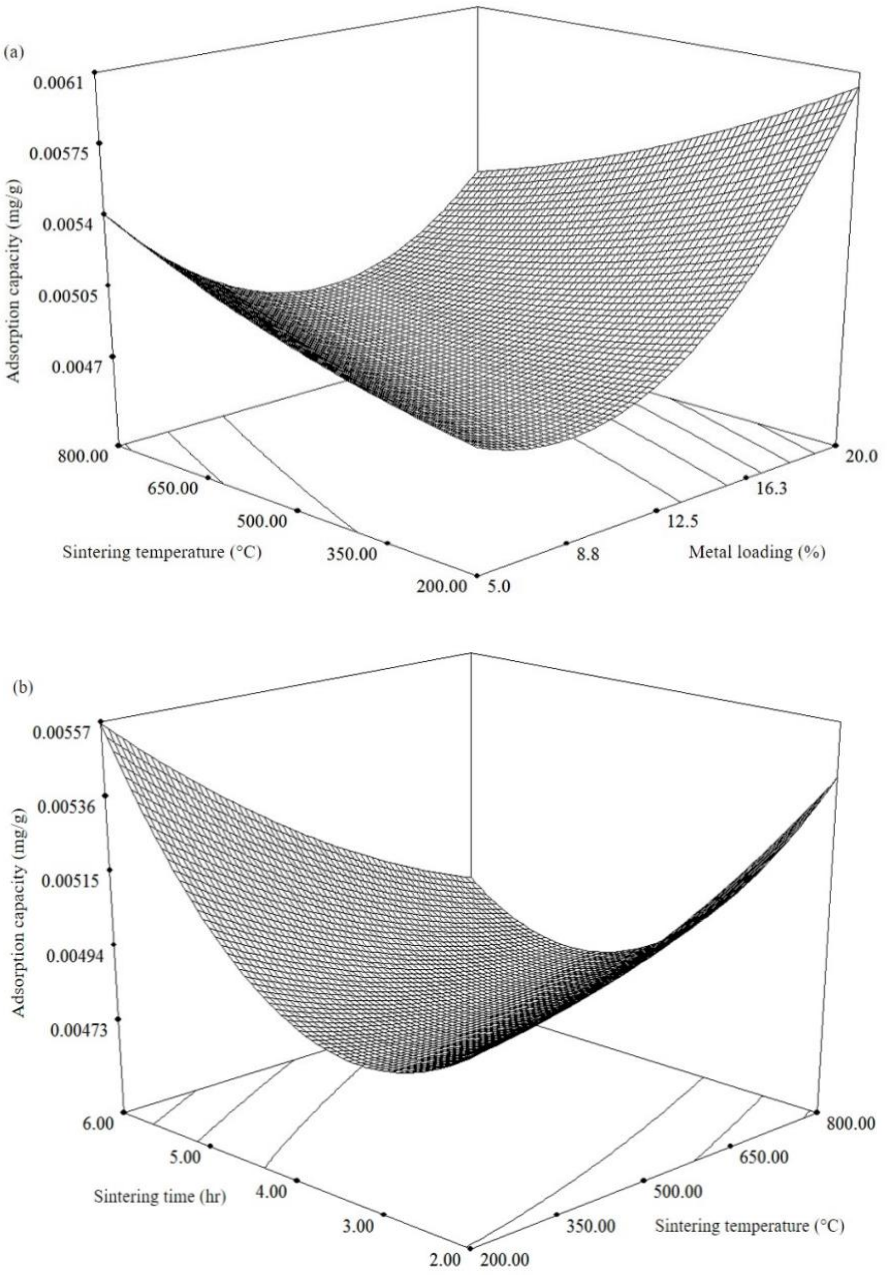

Fig. 2. Three-dimensional response surface plots of NO adsorption capacity by CuO/EFBC due to: (a) interaction between sintering temperature and metal loading, while the sintering time was set constant at 4 hrs; and (b) interaction between sintering time and sintering temperature, while the metal loading was set constant at 12.5%.

3.3 Model optimisation and validation

Model optimisation was carried out over selected range of operating variables for CuO impregnation to obtain CuO/EFBC with optimum NO adsorption capacity. By using Design-Expert software, a set of solution was generated by maximizing NO adsorption capacity and setting the individual variables, x_1, x_2 and x_3. Based on our results and support from literature [20-21], it is known that higher metal loading and lower sintering temperature is significant for NO removal, while prolonged sintering time increases the catalytic active sites of catalyst for the removal of NO. Thus, to achieve maximum NO adsorption capacity. the variables goal of the experimental model were set to be maximum for metal loading whereas the sintering temperature and sintering time were set to be minimum and maximum respectively.

With the optimized variables condition i.e. 20% metal loading, 200˚C sintering temperature and 6 hours sintering time, the model predicted an NO adsorption capacity of 0.00694 mg/g, as shown in Table 4. Experimental validation of the NO adsorption capacity predicted by the model results in adsorption capacity of 0.00680 mg/g, with only small error of 2%. Therefore, the model and optimum operating variables developed can be considered valid and applicable for predicting the response.

Table 4. Model validation for activated carbon prepared for NO adsorption.

Carbon supported catalyst	Model desirability	Metal Loading	Sintering temperature	Sintering time	NO adsorption capacity (mg/g)		
					Predicted	Experimental	Error
CuO/EFBC	0.9265	20%	200˚C	6 hours	0.00694	0.00680	2%

4 Conclusions

A quadratic model was developed using response surface methodology (RSM) with Box-Behnken Design for optimisation of selected CuO impregnation variables for enhancement of NO removal by CuO/EFBC. The model and variables i.e. metal loading, sintering time and sintering temperature of CuO impregnation was found to be significant in enhancing NO adsorption capacity (NO removal) through analysis of variance (ANOVA). The model term which has the most significant effect on the response is x_1^2 with an F-value of 50.64 and the overall effects are in the order of $x_1^2 > x_3^2 > x_1x_2 > x_1 > x_2x_3$. The interaction between high metal loading and low sintering temperature was noted to be most effective in enhancing NO adsorption capacity, followed by the interaction between high sintering time and low sintering temperature. The optimum operating variables for CuO impregnation onto EFBC at metal loading of 20%, sintering temperature of 200ºC and sintering time of 6 hours resulted in predicted NO adsorption capacity of 0.00694 mg/g. Experimental validation of the NO adsorption capacity shows good agreement with the model prediction, with only 2% errors.

The authors would like to acknowledge the support from the Fundamental Research Grant Scheme (FRGS) under a grant number of FRGS/2/2013/SG01/UNIMAP/02/1 from the Ministry of Higher Education Malaysia.

References

1. P. Nowicki, M. Skrzypczak, R. Pietrzak, Chem. Eng. J. **162**, 2, 723 (2010).
2. S. Sumathi, S. Bhatia, K. T. Lee, A. R. Mohamed, Chem. Eng. J. **162**, 1, 51 (2010).
3. X. Li, Z. Dong, J. Dou, J. Yu, A. Tahmasebi, Fuel Process. Technol. **148**, 91 (2016).
4. N. Md-Desa, Z. Ab Ghani, S. Abdul-Talib, C. Tay, Malaysian J. Anal. Sci. **20**, 3, 461 (2016).
5. I. Ghouma, M. Jeguirim, S. Dorge, L. Limousy, and A. Ouederni, C.R. Chim. **18**, 2, 63 (2015).
6. O. A. Bereketidou, N. D. Charisiou, M. A. Goula, *13th International Conference of Environmental Science and Technology*, Athens, Greece (2013).
7. J. M. Rosas, R. Ruiz-Rosas, J. Rodríguez-Mirasol, T. Cordero, Catal. Today **187**, 1, 201 (2012).
8. P. Nowicki, H. Wachowska, R. Pietrzak, J. Hazard. Mater. **181**, 1–3, 1088 (2010).
9. H. H. Tseng, C. Y. Lu, F. Y. Chang, M. Y. Wey, H. T. Cheng, Chem. Eng. J. **169**, 1–3, 135 (2011).
10. N. Ahmad, N. Ibrahim, U. F. M. Ali, S. Y. Yusuf, F. M. Ridwan, Procedia Eng. **148**, 823 (2016).
11. Z. Zhu, Z. Liu, S. Liu, H. Niu, T. Hu, T. Liu, Y. Xie, Appl. Catal. B **26**, 25 (2000).
12. H. Tseng, M. Wey, Y. Liang, K. Chen, Carbon **41**, 1079 (2003).
13. S. A. Pasma, R. Daik, M. Y. Maskat, O. Hassan, Int. J. Polym. Sci. **2013**, 8 (2013).
14. Y. S. Mohammad, S. B. Igboro, A. Giwa, C. A. Okuofu, J. Eng. **2014**, ID 278075 (2014).
15. M. Dutta, P. Ghosh, J. K. Basu, Appl. Sci. Res. **4**, 2, 1053 (2012).
16. J. M. Salman, Arab. J. Chem. **7**, 1, 10 (2014).
17. M. H. Kalavathy, I. Regupathi, M. Ganesa, L. Rose, Colloids Surf. B **70**, 35 (2009).
18. S. K. Ryu, W. K. Lee, S. J. Park, D. D. Edie, Accessed online at url: http://acs.omnibooksonline.com/data/papers/2004_L008.pdf (2004).
19. Z. H. Zhu, L. R. Radovic, G. Q. Lu, Carbon **38**, 3, 451 (2000).
20. G. Yang, Adv. Mater. Res., **428**, 61 (2012).
21. K. H. Chuang, Z. S. Liu, M. Y. Wey, Mater. Sci. Eng. B, **175**, 2, 100 (2010).